Journal of Optoelectronics and Advanced Materials Vol. 6, No. 1, March 2004, p. 269 - 276

TRANSPORT PROPERTIES OF $(Nd_{0.67}In_{0.33})_{1-x}Sr_xMnO_{3\pm\delta}$ COMPOUNDS

N. Cornei[a], M. -L. Craus[b*]

[a]University “Al. Cuza”, Faculty of Chemistry, Blvd. Carol I 11, 700506 Iasi, Romania
[b]National Institute for Research and Development for Technical Physics - TPI Iasi,
Blvd D. Mangeron 47, 700050 Iasi, Romania

The structure, magnetic and transport characteristics of $(Nd_{0.67}In_{0.33})_{1-x}Sr_xMnO_{3\pm\delta}$ compounds (where $x = 0.2$, 0.35 and 0.50), obtained by sol-gel method, were investigated between 77 and 600 K. It was observed that: (1) cubic and tetragonal phases appear for $x=0.2$ and, respectively, $0.2 < x \leq 0.5$, (2) there is a significant increase of the chemical disorder, accompanied by a decrease of the observed tolerance factor with the Sr concentration, (3) for Sr concentration corresponding to $x = 0.5$ the specific magnetic moment of the sample sharply decreases (more than ten times) and (4) the transition temperature from the metallic to the semiconductor state decreases with the increase in Sr concentration in the samples.

(Received October 6, 2003; accepted after revision March 9, 2004)

Keywords: Rare-earth manganites, Sol-gel method, X-ray, Specific magnetization, Transport phenomena

1. Introduction

The magnetoresistance effect is associated with a large decrease in the resistance by application of an external magnetic field and may be observed in some magnetic perovskites near the Curie temperature. Manganese perovskite oxides, with the general formula $A_{1-x}B_xMO_{3\pm\delta}$ (where A = Nd or In, and B = Sr) exhibit interesting magnetic and electric properties, such as a transition from insulator antiferromagnetic to metallic ferromagnetic behaviour, including colossal magnetoresistance (CMR) and charge ordering phenomena [1-3]. The magnetic and electrical properties have been explained within the framework of Zener double exchange theory [4], which considers the transfer of electrons between neighbouring Mn^{3+}–Mn^{4+} ions through Mn–O–Mn bonds. A strong magnetic field aligns the atomic magnetic moments, which enhances e_g electron hopping and reduces resistivity. The strong electron-phonon interactions due to the Jahn-Teller effect of the Mn^{3+} ions are greatly involved in the metallic-insulator transitions in manganites [5]. Magnetic superlattice can give new and essential way to control these spin ordered states directly.

The superexchange interaction, which describes interaction between localized spin moments, is essential for magnetism in transition metal oxides [6]. According to Goodenough-Kanamori rules, this mechanism gives rise to an antiferromagnetic interaction between cations with the same kind of *d*-shell and a ferromagnetic interaction between cations with more than half-filled *d*-shell and less than half-filled *d*-shell [7].

The ferromagnetic Curie temperature is related to the strength of the transfer integral t_{ij} between Mn^{3+}/Mn^{4+} ions, which itself controls the electronic (hole) conductivity. It follows that in this system one should expect a strong interplay between magnetic, transport and structural properties.

The aim of this work is to study the influence of the structural transformations on the interaction between the magnetic cations, in particular, the change in the magnetic properties and

---

[*] Corresponding author: craus@phys-iasi.ro; kraus@nf.jinr.ru; actual address: Joint Institut for Nuclear Research, Frank Laboratory of Neutron Physics, Joliot-Curie 6, 141980 Dubna, Moskovskaia obl., Russia

transport characteristics produced by the substitution of Sr with Nd and In in the $(Nd_{0.67}In_{0.33})_{1-x}Sr_xMnO_{3\pm\delta}$ system.

2. Experimental

$(Nd_{0.67}In_{0.33})_{1-x}Sr_xMnO_{3\pm\delta}$ manganites (where $x = 0.2$, 0.35 and 0.50) were synthesized by sol-gel method and finally sintered at 1200ºC in O_2 atmosphere for 5 hours. The oxides and acetates were dissolved in aqueous nitric acid solution and, respectively, in an aqueous acetic acid solution. Then the precursors were mixed in corresponding ratios and the gel was carried out using citric acid solution. The manganese cations were reduced to the bivalent state by dropping a small amount of hydrazine hydrate. The details of the samples preparation have been reported elsewhere [8, 9].

The oxygen content of the samples, which we consider that has a fixed cation stoichiometry, was determined by taking account of the manganese oxidation. We used a modified iodometric technique: 1) the samples were dissolved in concentrated HCl; 2) the resulted chlorine was absorbed by a KI solution; 3) the titration was made by using a 0.005 N standard sodium thiosulphate solution [10]. The errors in the determination of the oxygen content are caused from titration procedures.

The presintered and sintered samples were investigated by X-ray diffraction using a DRON 2,0 diffractometer with Co$K\alpha$ radiation and attached to a data acquisition system. Zero shift and specimen displacement corrections were introduced. Lattice constants and space group were determined and tested by using TREOR, DICVOL and, respectively, Ceckcell programs [11,12,13].

We made a preliminary attempt to determine the position of oxygen anions in the unit cell and of the temperature factors and used the results to determine the distances cation-anion and the Mn-O-Mn bond angle. The final crystallographic data concerning the structure of the $(Nd_{0.67}In_{0.33})_{1-x}Sr_xMnO_{3\pm\delta}$ system will be published elsewhere.

The calculated and observed tolerance factor were determined with the formulas:

$$t_{calc} = \frac{r_A + r_O}{\sqrt{2}(r_B + r_O)} \tag{1}$$

and

$$t_{obs} = \frac{d_{A-O}}{\sqrt{2}d_{Mn-O}} \tag{2}$$

due to Jonker [14] and, respectively, Cherif et al. [15].

The average radii of A and B places, r_A and, respectively, r_B were calculated with the formulas:

$$r_A = (0.67r_{Nd} + 0.33r_{In})(1-x)+xr_{Sr} \tag{3}$$

$$r_B = r_{Mn3+}\, y + r_{Mn4+}\, (1-y) \tag{4}$$

where r_{Nd} , r_{In} and r_{Sr} represent the radii of Nd^{3+}, In^{3+} and, respectively, Sr^{2+} cations on the A sites (12-fold coordination). As cationic radii we used the data of Huheey et al. [16].

The chemical disorder factor, σ, were calculated with [15]:

$$\sigma^2 = \sum C_i r_i^2 - r_A{}^2 \tag{5}$$

where C_i is the concentration of the cation with r_i radius.

The variation of the specific magnetization with temperature, Curie temperature and unit cell magnetization were determined by using a Foner-type magnetometer with a data acquisition system, which worked between 77 and 550 K, in a 0.5 T magnetic field. The system was calibrated by using a Ni sphere (Erba-Italy). The electric measurements were made on cylindrical samples of 10 mm diameter and about 1.5 mm height, with Ag covered basis, using a four-probe method and a data acquisition system.

3. Results and discussion

The compound with $x = 0.2$ has cubic structure (Pm3m, space group 221), while compounds with $x = 0.35$ and $x = 0.50$ have tetragonal structure (I4/mcm, space group 140) (see Fig. 1 and Table 1). The unit cell volume of the tetragonal phase decreases with an increase in Sr concentration in the sample. The split between the (004) and (220) maxims of the tetragonal phase and the c/a ratio increase with the Sr concentration (see Fig.1 and Table 1).

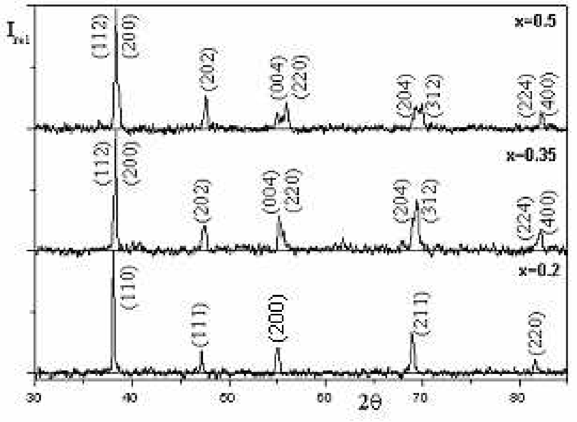

Fig. 1. Diffractograms of the $(Nd_{0.67}In_{0.33})_{1-x}Sr_xMnO_{3\pm\delta}$ manganites. The sintering was performed at 1200 °C.

Table 1. Lattice parameters (a, b, c), unit cell volume (V), calculated and observed tolerance factor (t_{cal}, t_{obs}) for the $(Nd_{0.67}In_{0.33})_{1-x}Sr_xMnO_{3\pm\delta}$ manganites,

x	Unit cell	a (Å)	b (Å)	c (Å)	V (Å^3)	t_{cal} 3)	$t_{obs.}$ 4)
0.2	C 1)	3.8459	3.8459	3.8459	56.88	0.949	0.999
0.35	T 2)	5.4372	5.4372	7.6151	225.13	0.972	0.958
0.5	T 2)	5.3562	5.3562	7.6935	220.72	0.996	0.956

1) cubic structure; 2) tetragonal structure; 3) calculated by using the Huheey et al. [16] radii with (1); 4) determined with eq. (2) from the experimental data concerning the average distances between A and O and, respectively, Mn and O.

From the preliminary data concerning the position of the O2 oxygen anion in the unit cell, we calculated the Mn-O distances between the closest Mn and O ions in the [001] direction and in the (110) plane and the values of Mn-O-Mn bond angle, for different Sr concentrations. The following features emerge:

(1) The bond Mn-O2-Mn angle in the (ab) (or (110)) crystallographic plane decreases, while the Mn-O1-Mn angle remains constant with the Sr concentration in the sample (s.Tab.2);

(2) The Mn-O distances on the [001] (or c) direction and those on the (ab) plan have, respectively, a minimum and a maximum against Sr concentration. The MnO_6 octahedron has a maximum distortion at $x = 0.35$.

An increase of the Sr concentration is associated with the increase of the r_A (average radius of A places), because the Sr cations have a larger radius than Nd and In cations, and a decrease of the r_B (average radius of B places), due to the decrease of the Mn^{3+}/Mn^{4+} concentration ratio. The observed volume/molecular unit (i.e. volume divided by the number of molecule per unit cell) and the t_{obs} decrease, in agreement with the decrease of the distortions induced by the Jahn-Teller effect of Mn^{3+} cations. It represents a better accommodation of the structure to the atoms that form the unit cell. The increase of the t_{calc} values and the decrease of the Mn^{3+} concentration, which is associated with a large Jahn-Teller distortion, with the substitution of the rare earth cations with Sr cations should lead to a less distorted lattice. However, the concentration of the cationic vacancies, calculated on the cation and oxygen concentration (see Table 1), decreases when the Sr concentration increases. Despite its, the level of the distortion of the real lattice and calculated chemical disorder degree, σ, increase, while the observed tolerance factor decreases (see Tables 1 and 2).

In the $AMnO_3$ perovskites, where A can be one or more rare earth element(s), partially substituted by an alkaline earth (Sr, Ca or Ba), Mn cations are surrounded by six O^{2-} anions. The octahedral crystalline field can lift the degeneracy of the 3d electrons by splitting the 3*d* level in a three state level (t_{2g}) and a two state level (e_g). The t_{2g} electrons have strongly correlated local spins even in the metallic state, the total spin of the t_{2g} electrons being S = 3/2. A strong Hund correlation exists between the t_{2g} and e_g possible itinerant electrons [17].

The appearance of the magnetism in the manganites with the perovskite structure can be due to interplay between the superexchange and double exchange interactions. The double exchange interaction (DE) is associated with the e_g (Mn)-$2p_\sigma$(O)-e_g (Mn) overlap, while the superexchange (SE) interaction is due to the t_{2g} (Mn)-$2p_\pi$(O)- t_{2g} (Mn) overlap. The e_g, $2p_\sigma$, t_{2g}, $2p_\pi$ etc. terms were explicitly presented in a review by Tokura and Tomioka [17]. It is expected that the AFM interaction (superexchange interaction) to be less influenced by the change in the angle of the Mn-O-Mn bond as the ferromagnetic (double exchange (DE)) interaction. The decrease in the average radii of A sites leads to a decrease of the Mn-O-Mn bond angle in (*ab*) crystallographic plane, associated with a decrease in the ferromagnetic interaction [18].

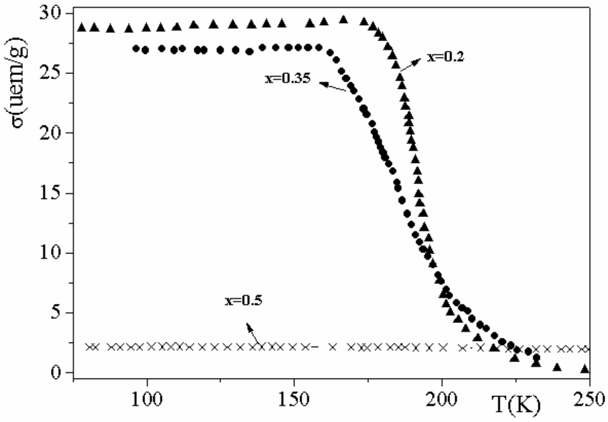

Fig. 2. The specific magnetization vs. temperature of the $(Nd_{0.67}In_{0.33})_{1-x}Sr_xMnO_{3\pm\delta}$ manganites. The sintering was made at 1200 °C; (1) x = 0,2; (2) x = 0.35; (3) x = 0.5.

The average radius of A places, r_A, calculated with Eq. (3), by using cationic radii corresponding to the A place coordination [16], increases monotonously with increasing Sr concentration from 143.1 to 148.7 pm. The calculated values of r_A for $Nd_{1-x}Sr_xMnO_3$ manganites increase also monotonously from 144.4 to 149.5 pm, when x changes from x = 0.2 to 0.5. For the $Nd_{1-x}Sr_xMnO_3$ manganites $T_C \approx a+bx$ (a, $b>0$; $x \in (0.1 \div 0.4)$) and $T_C \approx a' + b'x$ ($a>0$, $b<0$; $x \in (0.45 \div 0.55)$, that means an increase of T_C with Sr concentration for $x \in (0.1 \div 0.4)$ and, a decrease of T_C for $x \in (0.45 \div 0.55)$, respectively; between $x \approx 0.4$ and $x \approx 0.45$ the Curie temperature remains practically independent of the Sr concentration (see Fig. 6 of Tokura and Tomioka [17]). The variation of the Curie temperature with Sr concentration for the $(Nd_{0.67}In_{0.33})_{1-x}Sr_xMnO_{3\pm\delta}$ manganites is different from that of $Nd_xSr_{1-x}MnO_{3+\gamma}$. Starting from the observed Curie temperatures (see Table 2) we consider that the substitution of Nd with In leads to a change in the position of the maximum in Curie temperature (T_{Cmax}) to a lower value of the Sr concentration, probably near x ≈ 0.27, and to a lower value of T_{Cmax} (about 215 K) for the $(Nd_{0.67}In_{0.33})_{1-x}Sr_xMnO_{3\pm\delta}$ manganites, as compared with the T_{Cmax} value found for $Nd_{1-x}Sr_xMnO_3$ manganites (about 280 K for $x \approx 0.42$). This difference may be attributed to a decrease in the average radius of A site, because the radius of In cation is smaller than than that of Nd cation (see Refs. [19,20]).

The substitution of Nd by In enhances the chemical disorder and the local fluctuation in Mn-O distances and Mn-O-Mn bond angles. The increase in the chemical disorder and the decrease in the Mn-O-Mn bond angles accompanied by the increase of the Mn-O distances in the (*ab*) crystallographic planes, leads to a decrease in the double exchange interaction relative to superexchange interaction and destabilizes the ferromagnetic state. Consequently, the sample corresponding to $x = 0.5$ is mainly in paramagnetic or CE antiferromagnetic state and is characterized by a practically no specific magnetization (see Table 2).

From the observed value of the specific magnetization for $x > 0.35$ an apparent transition from the ferromagnetic to the antiferromagnetic structure takes place (cf. Table 2). The specific magnetization of the samples with $x < 0.5$ remains practically unchanged below the Curie temperature, showing a quick saturation at relatively low magnetic fields. A magnetic field of about 0.3 T is sufficient to saturate $(Nd_{0.67}In_{0.33})_{1-x}Sr_xMnO_{3\pm\delta}$ manganites, while the $Nd_{1-x}Sr_xMnO_{3\pm\delta}$ samples without In, with similar Sr concentration, attain saturation at much higher fields [21]. Some $Nd_{1-x}Sr_xMnO_{3\pm\delta}$ samples, sintered at about 1350°C, show a relaxation of the magnetic moment with temperature and treatment duration [22]. For an applied magnetic field up to 1T this type of behaviour was not observed for our samples. In agreement with the decrease of the Mn^{3+}/Mn^{4+} concentration ratio a monotonous increase of the specific magnetization should take place (see p_{calc} values in Table 2). The observed specific magnetization (p_{obs}) somewhat decreases when Sr concentration varies from $x = 0.2$ to $x = 0.35$, while it approaches practically zero for $x > 0.35$, as shown in Fig. 2 and Table 2. This behaviour may be attributed to a sudden change in the Mn-O distances and the angles of the Mn-O-Mn bonds.

Because a large difference exists between the calculated and the observed molecular magnetization, we suppose that the investigated samples have two components, characterized by the same crystallographic structure, but in two different magnetic states: ferromagnetic and non-magnetic states. The concentration of the magnetic state changes slowly with the Sr concentration up to $x = 0.35$. For the larger values of Sr concentration a sudden decrease of the specific magnetization of the samples can be observed (see Fig. 2 and Table 2). The ferromagnetic state must contain equal concentration of Mn^{3+} and Mn^{4+} cations, because the double-exchange interaction, implicitly the ferromagnetism of manganites, is based on the existence of the Mn^{3+}-O-Mn^{4+} type bond. The CE antiferromagnetic state can contain only Mn^{3+} or Mn^{4+} cations, bounded by a superexchange interaction as Mn^{3+}-O-Mn^{3+} etc. If the magnetic moments of the Mn^{3+} and Mn^{4+} only are taken into account, the calculated magnetic moments of the ferromagnetic phase are smaller than the observed values (see Table 2). We supposed that the magnetic moments of Mn cations are situated in the (*ab*) plane and are inclined with respect to the direction of the total magnetic moment of the samples. However, in this case the variation of the observed magnetic moment is determined by the Mn^{4+} concentration, implicitly by the Mn^{3+}-Mn^{4+} pair concentration, and by the angle between the atomic magnetic moments. If we compare the calculated and observed molecular magnetic moments (see Table 2), one finds that the angle between the magnetic moments of the Mn cations in the ferromagnetic phase increases with the Sr concentration from 162.28 to 178.37°.

Table 2. Curie temperature (T_C), transition temperature (T_t), observed molecular magnetization (p_{obs}), calculated molecular magnetization (p_{calc}), degree of chemical disorder (σ^2), Mn-O distances ($d_{Mn\text{-}O}$) and Mn-O-Mn angles ($\alpha_{Mn\text{-}O\text{-}Mn}$) for the $(Nd_{0.67}In_{0.33})_{1-x}Sr_xMnO_{3\pm\delta}$ manganites.

x	T_C (K)	T_t (K)	p_{obs} (μ_B)	p_{calc} (μ_B)	σ^2 (Å^2) ($\cdot 10^2$)	$d_{Mn\text{-}O1}$ (Å)	$d_{Mn\text{-}O2}$ (Å)	$\alpha_{Mn\text{-}O2\text{-}Mn}$ (°)	$\alpha_{Mn\text{-}O1\text{-}Mn}$ (°)
0.2	204	176	1.078	1.484	0.61	1.9230	-	180.00	180.00
0.35	213	133	1.044	2.522	0.83	1.9038	1.9361	166.32	180.00
0.5	< 77	< 77	0.100	3.502	0.90	1.9234	1.9312	157.38	180.00

O1 represents oxygen on (3d) in the P*m*3m lattice or (4a) position in the I4/mcm structure, for x>0.2, while O2 represent the oxygen on (8h) position for I4/mcm structure; p_{calc} was obtained taking account all parallel magnetic moments of the Mn^{3+}-Mn^{4+} pars.

From the data presented in Table 2 no direct relationship is evident between the variation of the Mn-O distances and the angle of the Mn-O-Mn bonds and the Curie temperature.

The increase of the Sr concentration in the samples leads to an increase in the average radii of A sites, implying a change in the Mn-O length bonds and a distortion of the MnO_6 octahedrons. However, an increase in the average radii of A sites should be associated with an increase in the angle of Mn-O-Mn bonds.

A decrease in the superexchange interaction can be attributed to a decrease in the Mn-O distances, in agreement with the literature [6]. A comparison of our data concerning the magnetic properties with those of Abramovich et al. [21] shows that the presence of In and Nd in the A lattice site leads to a higher local disorder of Mn-associated magnetic lattice, implying a relative increase in the superexchange as comparing with the double exchange interaction. The increase of the local disorder can be attributed to the difference between the ionic radius of Sr, on the hand, and the ionic radii of Nd and In, on another. Concerning the competition between the DE and SE interactions, we consider that the modifications of the Mn-O-Mn average angles, on the (*ab*) crystallographic plane, are associated with a decrease of the DE interactions as compared with the SE interaction, suggesting a change in the magnetic phase composition of the investigated manganites.

According to Frontera et al. [23] the magnetic structure of $Nd_{0.5}Ca_{0.5}MnO_{3+\delta}$ very strongly depends on the O content of the samples; the angle between the magnetic moment of the Mn cations increases from 130° to 180° (perfect CE antiferromagnetic structure), when the δ decreases from 0.04 to 0.2. In the model proposed by Frontera et al., the magnetic moments of the Mn cations are considered to be in the (*ac*) crystallographic plane [23]. A decrease of the oxygen content in the investigated $(Nd_{0.67}In_{0.33})_{1-x}Mn_xO_{3\pm\delta}$ manganites with an increase in Sr concentration could be also associated with a decrease in the angle between the direction of the magnetic moments of two neighbour Mn cations and a corresponding decrease in the specific magnetic moment of the samples.

Khiem et al. [24] found a monotonous dependence of Curie temperature on the average radius of the A places and chemical disorder. The dependence of the disorder degree on the Curie temperature means that the band width depends on the disorder (crystalline or chemical) degree. In view of the results of Khiem et al. [24], we suggest that the increase in the disorder degree leads to a decrease in the band width, and, consequently, to a decrease in the Curie temperature.

Concerning the disorder (crystalline or chemical) degree, we suppose that the crystallite is formed by two regions: (1) the core, with a high degree of order, associated with a higher band width and Curie temperature and (2) the boundary layer, characterized by a lower degree of order. The difference between the these two regions can be attributed to a different distribution of the cations in the crystallite and a higher crystalline and chemical disorder in the grain boundary.

The existence of zones with different degree of disorder in the crystallite leads to a change in the dependence of the specific magnetization and, specially, of the resistivity on temperature. A higher value of the specific magnetization implies a higher degree of order of crystalline and magnetic lattice, and, consequently, of the atomic magnetic moments. Its is expected that an increase of the crystalline disorder degree, connected with a higher chemical disorder degree, leads to a decrease of the specific magnetization, associated with the decrease of the angle between the magnetic atomic moments and the direction of the total magnetization, in agreement with Ref.22 and 23.

Accordingly to Zener [4], below the Curie temperature (T_C) the mobility μ of a charge carrier in the manganites may be given by

$$\mu = eD_0/kT, \tag{6}$$

where e is the electron charge, D_0 is the temperature-independent diffusion coefficient, k is the Boltzmann constant and T is the temperature in Kelvin. This relation predicts a linear dependence of resistivity on temperature (a metallic behaviour). An increase of the resistivity with temperature up to transition temperature was observed for $x \leq 0.35$, but the dependence is far from the Zener prediction, as seen from Fig. 3a. Above the Curie temperature, the dependence of the resistivity on temperature is characteristic of an insulator. The results concerning the physical model of resistivity behaviour with temperature and magnetic field will be published elsewhere.

The transition temperatures from the metallic to the insulator state decreases monotonously with an increase in Sr concentration in the samples (see Table 2). This observation is in agreement with the literature [21, 25, 26]. For samples with $x > 0.35$ the transition temperature (if any) is lower as 77 K, but the $(Nd_{0.67}In_{0.33})_{0.5}Sr_{0.5}MnO_{2.999}$ sample still exhibits a negative magnetoresistance behaviour. The $(Nd_{0.67}In_{0.33})_{0.8}Sr_{0.2}MnO_{3.006}$ sample has the highest transition temperature from metallic to the semiconductor state (see Fig. 3a). However, the magnetoresistance maximum increases with Sr concentration.

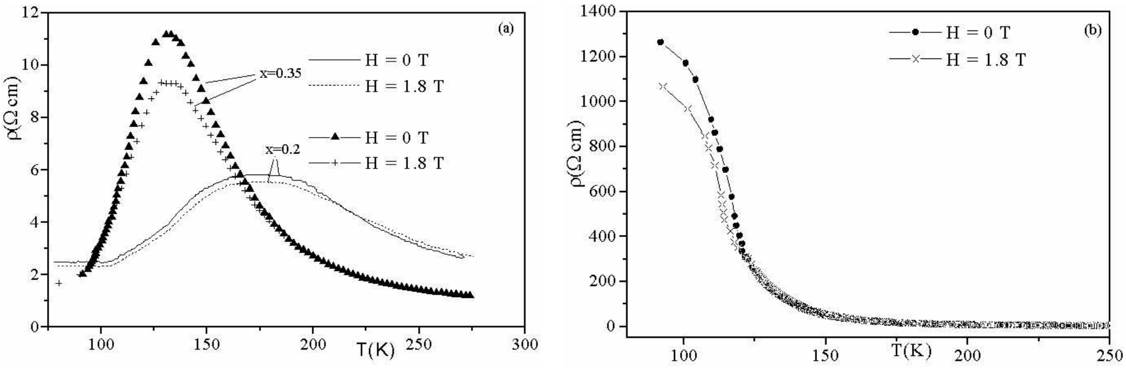

Fig. 3. Dependence of the resistivity of the $(Nd_{0.67}In_{0.33})_{1-x}Sr_xMnO_{3\pm\delta}$ manganites with the temperature and the intensity of the magnetic field. (a) $x = 0.20$ and 0.35; (b) $x = 0.50$.

For the investigated system the displacement of the transition temperature to lower values is bounded by an increase in the degree disorder of the crystallite with an increase in the Sr concentration. We take into account two components of the resistivity: one component due to the boundary layer, and the second due to the grain core. Both grain regions can exhibt a maximum in the plot of resistivity with temperature. The first component, due to the grain boundary, has a value much higher as that due to the core of the crystallite. The variation in the second component of the temperature dependence of resistivity, which supposes a maximum near the Curie temperature, was not observed for the $(Nd_{0.67}In_{0.33})_{1-x}Sr_xMnO_3$ system. However, the resistivity of the $(Nd_{0.67}In_{0.33})_{1-x}Sr_xMnO_3$ ($x = 0.2$ and 0.33) is in agreement with the values observed by Abramovich et al. [21] for the polycrystalline $Nd_{1-x}Sr_xMnO_3$ ($x = 0.33$ and 0.45) manganites, but is much higher as compared with that for the monocrystalline $Nd_{1-x}Sr_xMnO_3$ samples. It is known that in the monocrystalline manganites the resistivity is much lower than that of the corresponding crystalline samples, because the resistivity component due to the grain boundary disappears. Comparing our resistivity data with those of Caignaert et al. [27], we conclude that the observed values of the resistivity are mainly due to the grain boundary layer, which have a high degree of lattice distortions and chemical disorder.

4. Conclusions

We obtained for the first time the $(Nd_{0.67}In_{0.33})_{1-x}Sr_xMnO_3$ manganites by the sol-gel method and found a primitive cubic (Pm3m) and, respectively, a tetragonal (I4/mcm) structures, depending on the Sr concentration.

The concentration ratio of canted ferromagnetic and antiferromagnetic states determine the magnetic behavior. The extrinsic effects caused by the distorted layers of the crystallites and the Sr concentration rule over the transport characteristics. The ferromagnetic region in $(Nd_{0.67}In_{0.33})_{1-x}Sr_xMnO_3$ system is placed at lower Sr concentration as comparing with the $Nd_{1-x}Sr_xMnO_3$ system.

References

[1] C. N. R. Rao, A. K. Chettham, R. Mahesh, Chem. Mater. **8**, 2421(1996).
[2] Y. Moritomo, A. Asamitu, Y. Tokura, Phys. Rev. B **51**, 16491(1995).
[3] H. Tanaka, T. Kawai, J. Appl. Phys. **88**, 1559 (2000).
[4] C. Zener, Phys. Rev. **82**, 403 (1951).

[5] A. J. Millis, B. I. Shraiman and R. Mueller, Phys. Rev.Lett. **77,** 175 (1996).
[6] P. W. Anderson, Phys. Rev. **79**, 350 (1950).
[7] J. Kanamori, J. Phys. Chem. Solids **10**, 97 (1959).
[8] M.-L. Craus, N. Cornei, I. Berdan, C. Mita, M. N. Palamaru, Ceramics International, CERI 1549, in press corrected proof (2004).
[9] I. Berdan, N. Cornei, M. -L. Craus, C. Mîţă, Ann**.** St. Univ. "Al. I. Cuza"-Iasi **X(2)**, 167 (2002).
[10] I.G. Krogh Andersen, E. Krogh Andersen, P. Norby and E. Skou, J. Solid St. Chem. **113,** 320 (1994).
[11] A. Boultif and A. Louer, J. Appl.Cryst. **24**, 987 (1991).
[12] P.E.Werner, J. Appl.Cryst. **9**, 216 (1976).
[13] J. Laugier and B. Bochu, Checkcell, programme développed dans Laboratoire des Matériaux et du Génie Physique, Ecole Nationale Supérieure de Physique de Grenoble (INPG) http://www.inpg.fr/LMGP.
[14] G.H.Jonker, Physica **22**, 707 (1956).
[15] K.Cherif, J.Dhahri, E.Dhahri, M.Oumezzine and H.Vincent, J. Sol. State Chem. **163**, 466 (2002).
[16] J.E.Huheey, E.A.Keiter and R.I.Keiter, Chemistry. Principls of Structure and Reactivity, Ed. Harpers Collins, College Publishers (1993).
[17] Y. Tokura and Y. Tomioka, J. M. M. M. **200,** 1 (1999); T.Okuda, T. Kimura and Y. Tokura, Phys. Rev. B **60**, 3370 (1999).
[18] J. B. Goodenough, Annu. Rev. Mater. Sci. **28**, 1 (1998).
[19] T. Terai, T. Kakeshita, T. Fukuda, M. Yamamoto, T. Saburi, H. Kitagawa, K. Kindo, M. Honda, Trans. Materials Research Society of Japan **25**, 217 (2000).
[20] R. Mathieu, P. Svedlindh, P. Nordblad, Europhys. Lett. **52**, 441 (2000).
[21] A. I. Abramovich, A. V. Michurin, O. Yu. Gorbenko, A. R. Kaul, J. Phys.: Cond. Matter. **12**, L627 (2000).
[22] D. N. H. Nam, R. Mathieu, P. Nordblad, N. V. Khiem and N. X. Phuc, Phys.Rev. B **62,** 1027 (2000).
[23] C. Frontera, J.- L. Garcýa-Munoz, A. Llobet, C. Ritter, J.- A. Alonso, J. Rodrýguez-Carvajal, Phys. Rev. B **62,** 3002 (2000).
[24] N. V. Khiem, L.V. Bau, L. H. Son, N. X. Phuc and D. N. H. Nam, J. M. M. M. **262**, 490 (2003).
[25] K. H. Kim, J. Y. Gu, H. S. Choi, G. W. Park, T. W. Noh, Phys. Rev. Letters **77**, 1877 (1996).
[26] W. Boujelben, M. Ellouze, A. Cheikh-Rouhou, J. Pierre, Q. Cai, W. B. Yelon, K. Shimizu, C. Dubourdieu, J. Alloys Comp. **334**, 1 (2002).
[27] V.Caignaert, A.Magnan and B.Raveau, Sol. State Comm. **95,** 357 (1995).